Supporting Information

for

Crystal Structures and Magnetic Properties of a Set of Dihalo-Bridged Oxalamidato Copper(II) Dimers

Dijana Žilić,[a] Boris Rakvin,[a] Dalibor Milić,[b‡] Damir Pajić,[c] Ivica Đilović,[b] Massimo Cametti[d] and Zoran Džolić*[a]

[a] *Ruđer Bosković Institute, Bijenička cesta 54, 10000 Zagreb, Croatia; E-mail: Zoran.Dzolic@irb.hr*
[b] *Department of Chemistry, Faculty of Science, University of Zagreb, Horvatovac 102A, 10000 Zagreb, Croatia*
[c] *Department of Physics, Faculty of Science, University of Zagreb, Bijenička cesta 32, 10000 Zagreb, Croatia*
[d] *Department of Chemistry, Materials and Chemical Engineering "Giulio Natta", Politecnico di Milano, Via L. Mancinelli 7, 20131 Milano, Italy*
[‡] *Present address: Paul Scherrer Institut, 5232 Villigen PSI, Switzerland*

Table of content

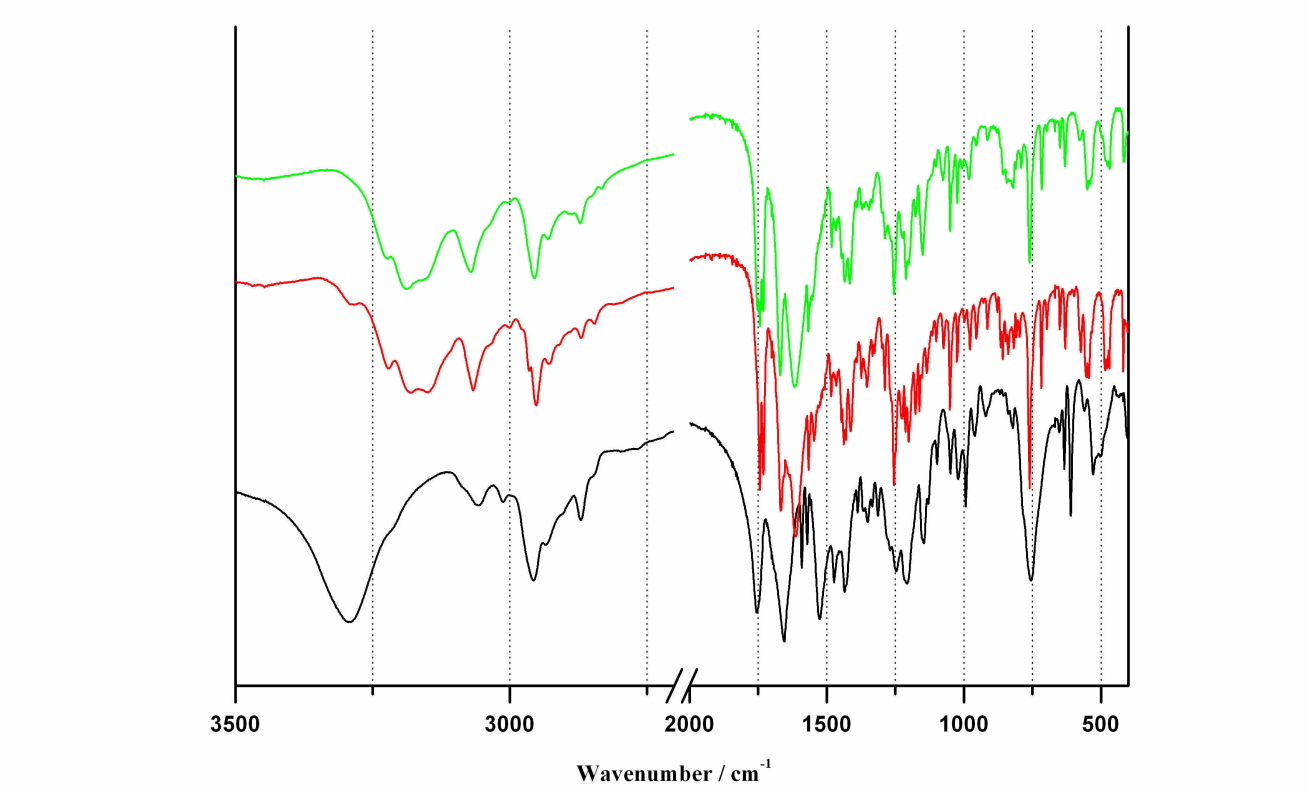

Fig. S1: FT-IR spectra of the ligand L^1 (black line) and complexes **L^1–Cl** (green line) and **L^1–Br** (red line).

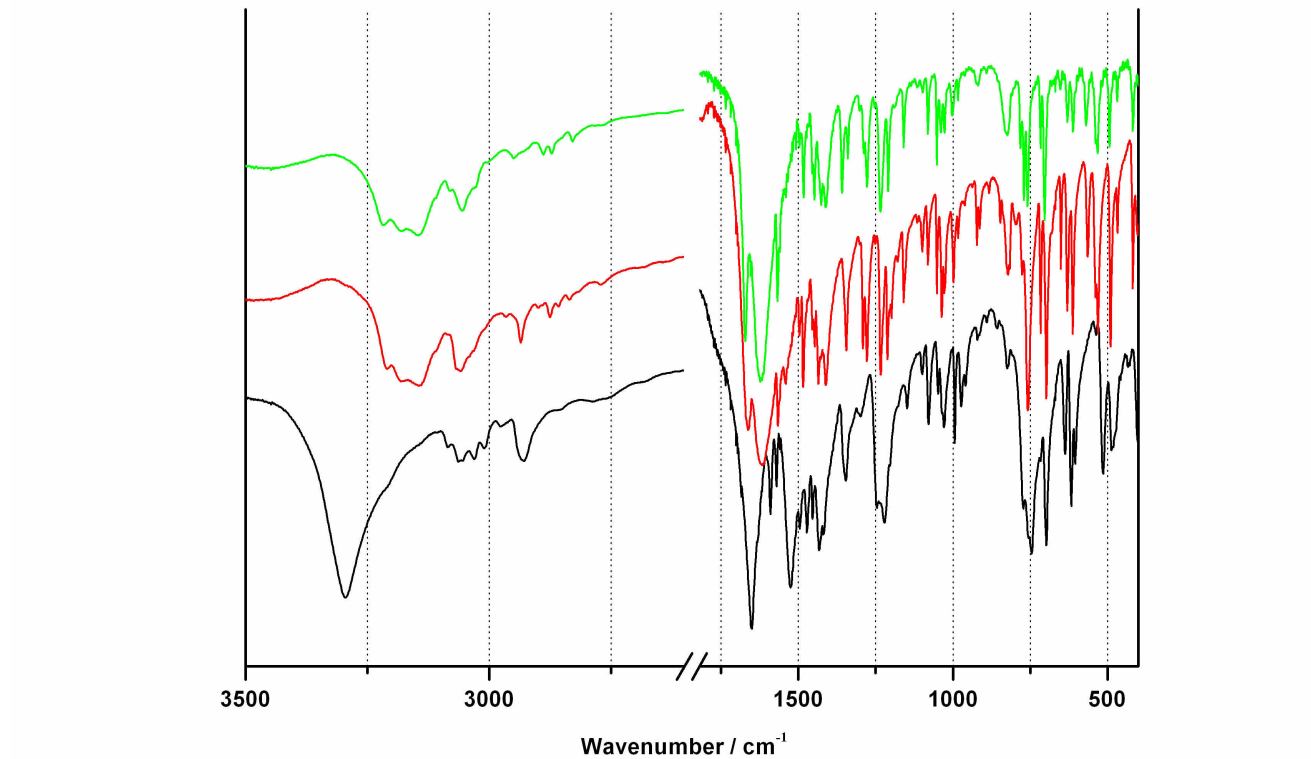

Fig. S2: FT-IR spectra of the ligand L^2 (black line) and complexes **L^2–Cl** (green line) and **L^2–Br** (red line).

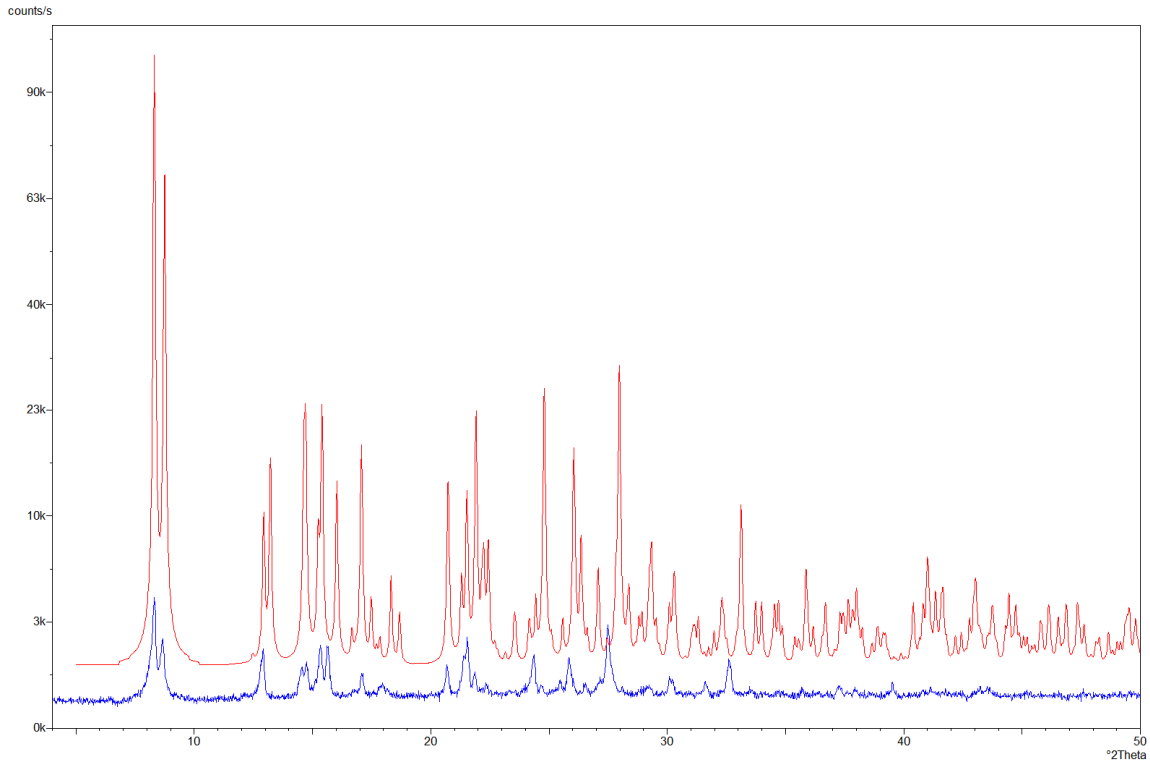

Fig. S3: Comparison between the measured (blue) and the calculated (red) powder diffraction patterns for $\mathbf{L^1}$**–Cl**.

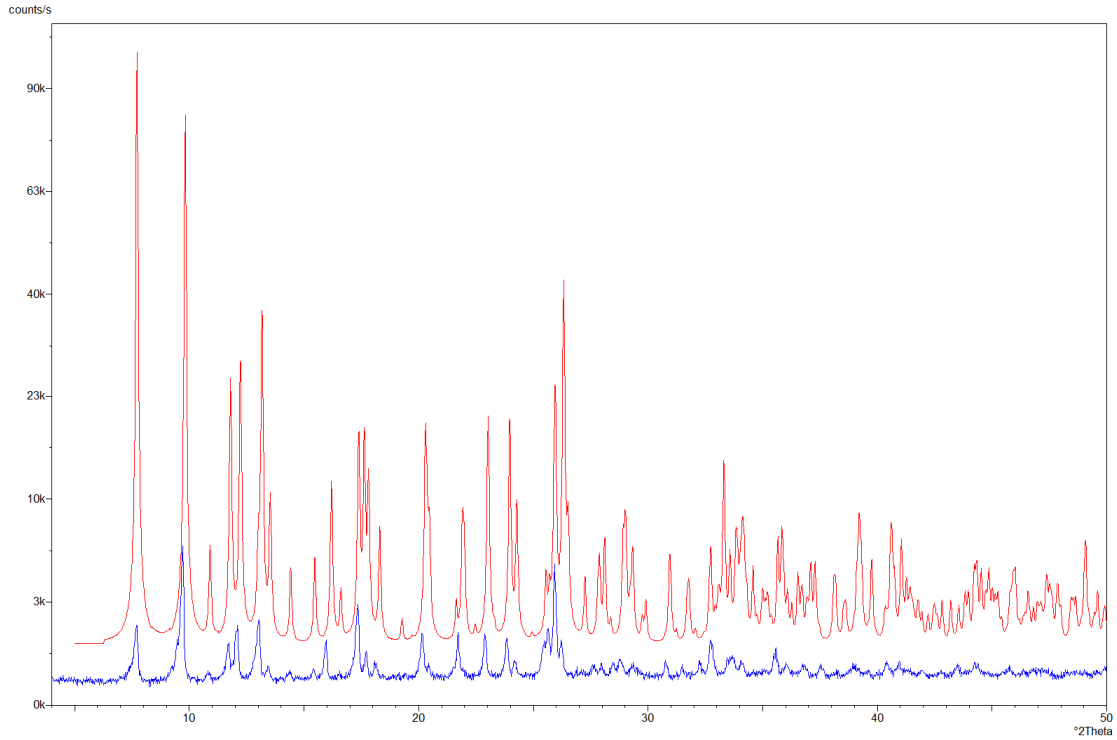

Fig. S4: Comparison between the measured (blue) and the calculated (red) powder diffraction patterns for $\mathbf{L^2}$**–Cl**.

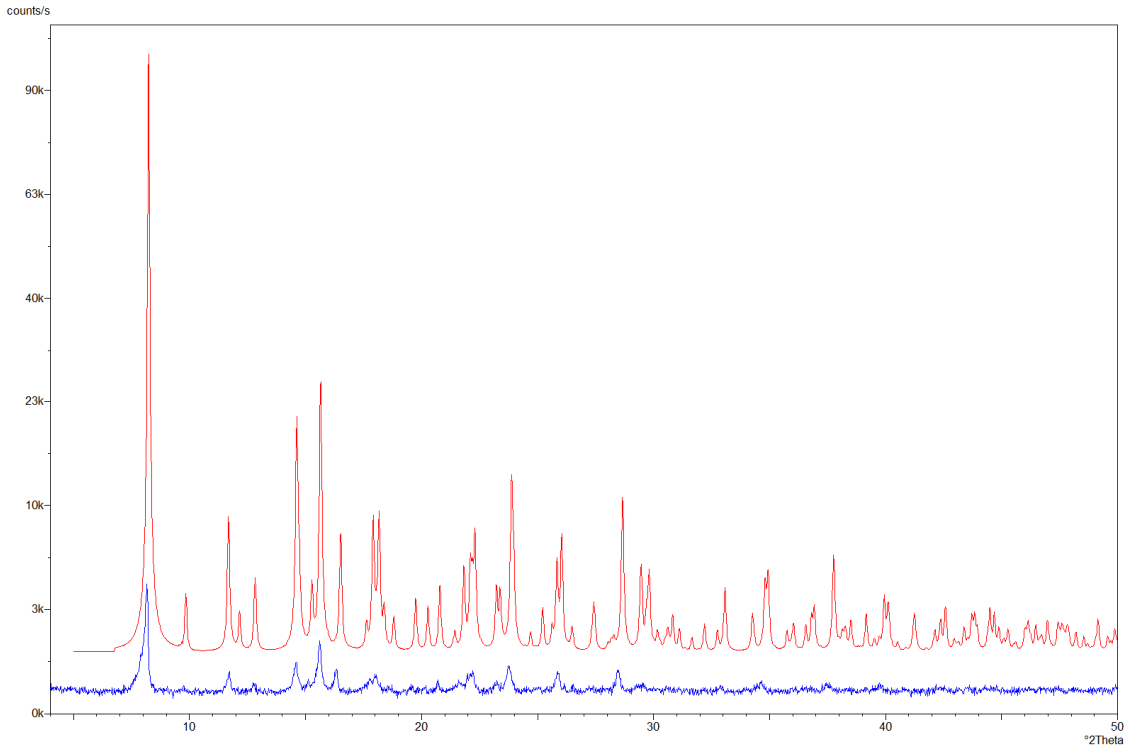

Fig. S5: Comparison between the measured (blue) and the calculated (red) powder diffraction patterns for **L^1–Br**.

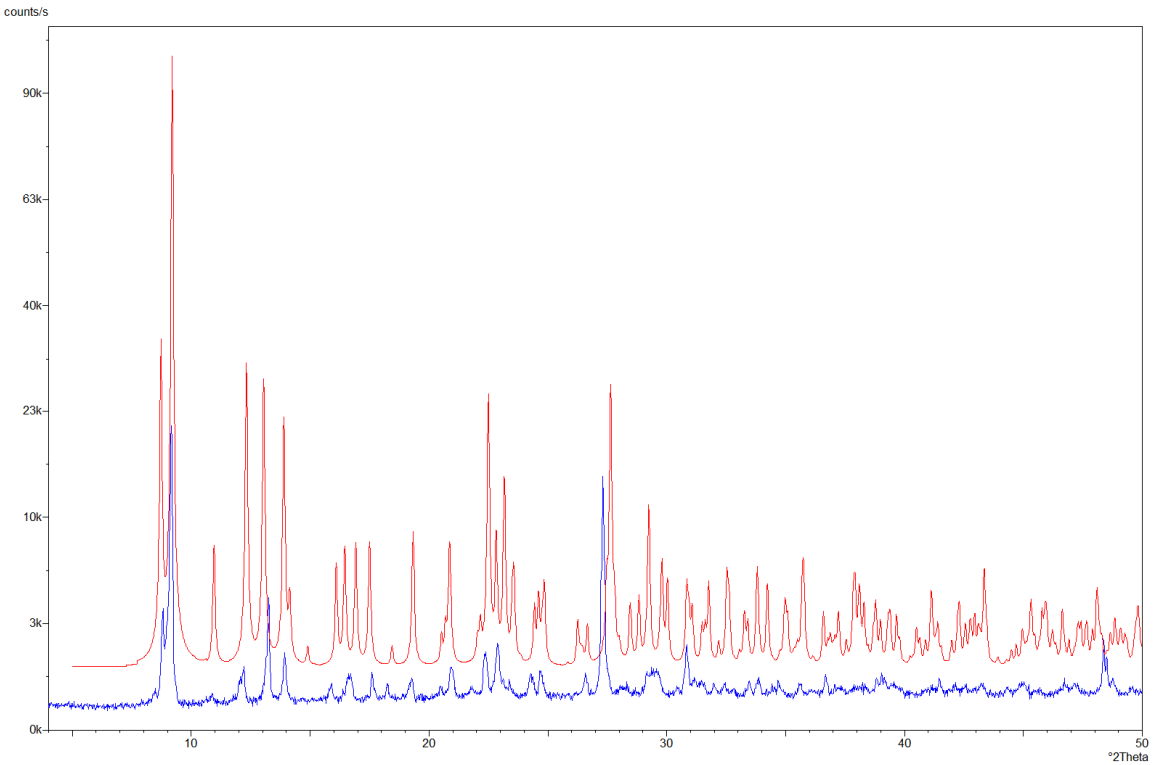

Fig. S6: Comparison between the measured (blue) and the calculated (red) powder diffraction patterns for **L^2–Br**.

Description of the Crystal Packing Interactions for L^2–Cl, L^1–Br and **L^2–Br.**

The crystal structure of **L^1–Cl** has been described in a previous occasion [Z. Džolić et al., *Chem.-Eur. J.*, 2013, **19**, 5411–5416]. Here, we provide a description of the crystal packing interactions observed in the three other complexes (**L^2–Cl, L^1–Br** and **L^2–Br)**. Complete atom numbering schemes are presented in Figures S7 and S8. Geometrical details of the hydrogen bonding, stacking and C–H···π interactions are given in Tables 5, 6 and 7, respectively.

A common structural motif present in all cases is constituted by an infinite chain of molecular dimers connected by N–H···O hydrogen bonds between the oxalamide groups (Figure 4 in the article). Other supramolecular structural features, instead, differ among the four crystal structures. In the structure of **L^2–Cl**, *N*-benzyl group are found having two different conformations, with the minor one (yellow in Figure S9) occurring in 16 % of monomers. The intramolecular C15A-H15A···O2 bonds form only when the *N*-benzyl group assumes the major conformation (gray in Figure S9). The dinuclear complexes are also linked by C–H···π interactions between the methylene groups and the metalloaromatic chelate rings as well as those between the pyridyl and the disordered *N*-benzyl units, regardless of which of the two possible conformation is adopted (Figure S9c). In addition to the characteristic N–H···O hydrogen bonds in **L^2–Cl**, there are also weak intermolecular C4–H4···Cl1 (– 1 – *x*, 2 – *y*, 1 – *z*) interactions (Figure S9b).

Stacking interactions between pyridine and metalloaromatic chelate rings play an important role in crystal packing of **L^1–Cl** as well as of both **L^1–Br** and **L^2–Br** dimers (Figures S10 and S11). Furthermore, these stacking interactions are accompanied with the C–H···O bonds between pyridyl moieties and the ester carbonyl O atoms of the two **L^1–Br** molecules stacked together (Figure 11b) or, in case of **L^2–Br**, C–H···π interactions involving a pyridyl *para* C–H and an *N*-benzyl aromatic ring (Figure S11b). In the structure of **L^1–Br**, a weak C–H···π interaction there also exists, but between methyl C28–H28C and the metalloaromatic chelate ring of the adjacent dimer (Figure S10). Moreover, **L^1–Br** and **L^2–Br** also possess other weak intermolecular C–H···*A* interactions, as detailed in Table 5 and illustrated in Figures S10 and S11. Surprisingly, π–π stacking interactions between aryl groups are only present in the structure of **L^2–Br** (Figure S11b).

Table 5 Hydrogen-bonding parameters (Å, °) in crystal structures of the studied complexes.

	D–H···*A*	*D*–H	H···*A*	*D*···*A*	*D*–H···*A*	Symmetry operator on *A*
L[1]–Cl	N3–H3N···O5	0.86(2)	2.08(3)	2.858(3)	150(2)	1 + *x*, 1 + *y*, *z*
	N6–H6N···O1	0.85(2)	1.99(3)	2.816(3)	163(2)	– 1 + *x*, – 1 + *y*, *z*
	O9–H9A···Cl2	0.84	2.46	3.256(5)	158	.
	C2–H2···O9	0.95	2.42	3.240(7)	144	1 + *x*, *y*, *z*
	C19–H19···O3	0.95	2.46	3.126(4)	127	– 1 + *x*, *y*, *z*
	C20–H20···Cl2	0.95	2.79	3.366(2)	120	.
	C25–H25A···O1	0.99	2.54	3.257(3)	129	– 1 + *x*, – 1 + *y*, *z*
L[2]–Cl	N3–H3N···O1	0.86(2)	1.96(2)	2.721(3)	147(2)	1 – *x*, 1 – *y*, 1 – *z*
	C15A–H15A···O2	0.95	2.50	3.183(5)	129	.
	C4–H4···Cl1	0.95	2.75	3.659(3)	162	– 1 – *x*, 2 – *y*, 1 – *z*
L[1]–Br	N3–H3N···O5	0.88	1.96	2.796(5)	159	1 + *x*, *y*, – 1 + *z*
	N6–H6N···O1	0.88	1.98	2.758(5)	146	– 1 + *x*, *y*, 1 + *z*
	C3–H3···O7	0.95	2.35	3.241(6)	157	1 + *x*, *y*, *z*
	C10–H10B···O5	0.99	2.46	3.101(5)	122	1 + *x*, *y*, – 1 + *z*
	C18–H18···O3	0.95	2.53	3.424(6)	156	– 1 + *x*, *y*, *z*
	C21–H21B···O7	0.99	2.46	3.404(5)	159	*x*, – 1 + *y*, *z*
L[2]–Br	N3–H3N···O1	0.88	2.09	2.802(6)	138	2 – *x*, 1 – *y*, 1 – *z*
	C6–H6A···Br1	0.99	2.87	3.750(5)	148	2 – *x*, 1 – *y*, – *z*

Table 6 Stacking interactions (Å, °) in the studied crystal structures.

	Ring *m*····Ring *n*[a]	*Cgm*···*Cgn*[b]	α[c]	Mean plane of Ring *m*···*Cgn*	Ring offset	Symmetry operator on ring *n*
L[1]–Cl	Ring 1····Ring 4	3.644(1)	4.9(1)	3.528(1)		1 + *x*, *y*, *z*
	Ring 2····Ring 3	3.647(1)	8.1(1)	3.542(1)		*x* – 1, *y*, *z*
L[1]–Br	Ring 1····Ring 4	3.675(2)	5.4(2)	3.482(2)		1 + *x*, *y*, *z*
	Ring 2····Ring 3	3.652(2)	6.8(2)	3.492(2)		*x* – 1, *y*, *z*
L[2]–Br	Ring 1···Ring 3	3.601(3)	5.7(2)	3.496(2)		2 – *x*, 1 – *y*, –*z*
	Ring 5···Ring 5	3.708(4)	0	3.566(3)	*ca.* 1.02	1 – *x*, – *y*, 1 – *z*

[a] Definition of the rings:
Ring 1 – metalloaromatic chelate ring Cu1/O2/C8/C7/N2;
Ring 2 – metalloaromatic chelate ring Cu2/O6/C23/C22/N5;
Ring 3 – pyridyl ring N1/C1–C5;
Ring 4 – pyridyl ring N4/C16–C20;
Ring 5 – phenyl ring C10–C15.

[b] *Cgm* and *Cgn* are centroids of the rings *m* and *n*.

[c] α is the dihedral angle between the mean planes of the two interacting rings (*m* and *n*).

Table 7 C–H···π interactions (Å, °) in the studied structures.

	D–H···*Cg*[a]	H···*Cg*	*D*···*Cg*	*D*–H···*Cg*	Symmetry operator on *Cg*
L^2–Cl	C2–H2···*Cg*5A	2.68	3.573(4)	156	– *x*, 1 – *y*, 1 – *z*
	C2–H2···*Cg*5B	2.82	3.527(7)	132	– *x*, 1 – *y*, 1 – *z*
	C6–H6B···*Cg*1	3.00	3.927(2)	157	– *x*, 1 – *y*, 1 – *z*
L^1–Br	C28–H28C···*Cg*1	2.95	3.586(5)	123	*x*, *y*, *z* + 1
L^2–Br	C3–H3···*Cg*5	2.58	3.464(6)	154	2 – *x*, 1 – *y*, –*z*
	C13–H13···*Cg*1	2.98	3.908(7)	167	*x*, *y* – 1, *z*

[a] Definition of the ring centroids:

*Cg*1 – metalloaromatic chelate ring Cu1/O2/C8/C7/N2;

*Cg*5 – phenyl ring C10A–C15A;

*Cg*5A – phenyl ring of **L^2–Cl** in the major disordered conformation C10A–C15A;

*Cg*5B – phenyl ring of **L^2–Cl** in the minor disordered conformation C10B–C15B.

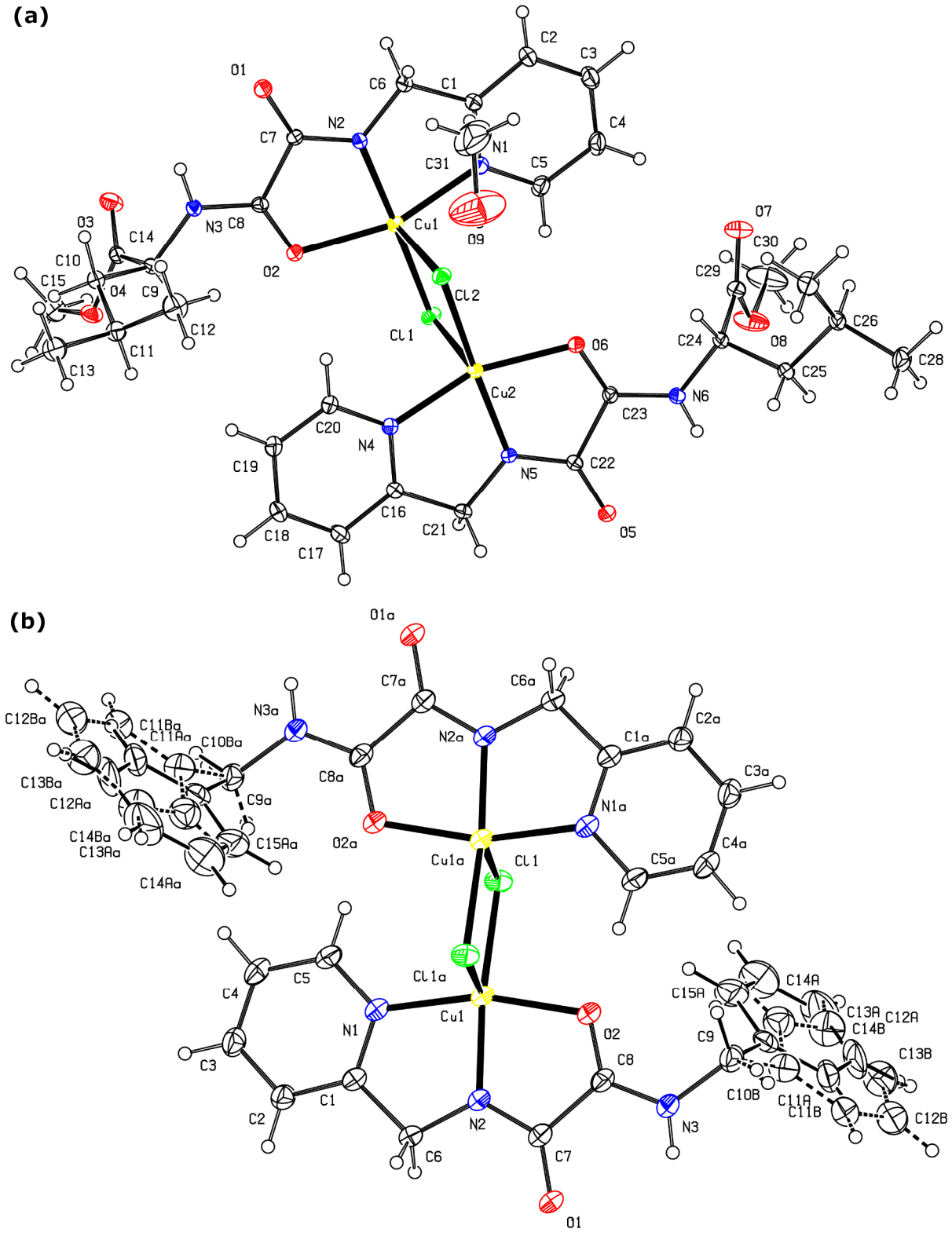

Fig. S7: Atom numbering schemes for (a) $\mathbf{L^1}$**–Cl** and (b) $\mathbf{L^2}$**–Cl**. Dashed lines represent the minor conformation of the disordered *N*-benzyl group. Atoms labelled with "a" in $\mathbf{L^2}$**–Cl** are centrosymmetrically related to those in the other half of a molecule.

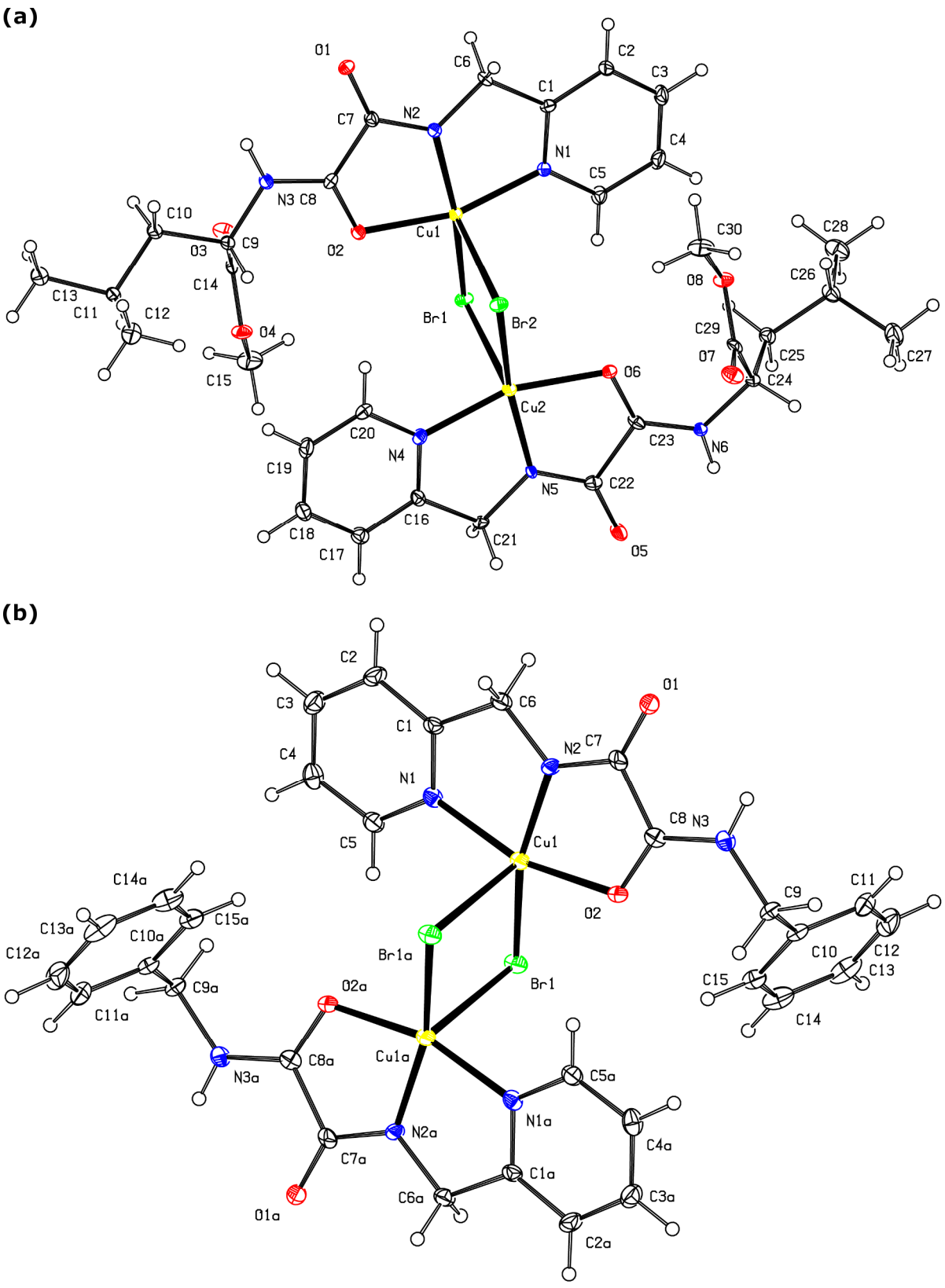

Fig. S8: Atom numbering schemes for (a) $\mathbf{L^1}$**–Br** and (b) $\mathbf{L^2}$**–Br**. Atoms labelled with "a" in $\mathbf{L^2}$**–Br** are centrosymmetrically related to those in the other half of a molecule.

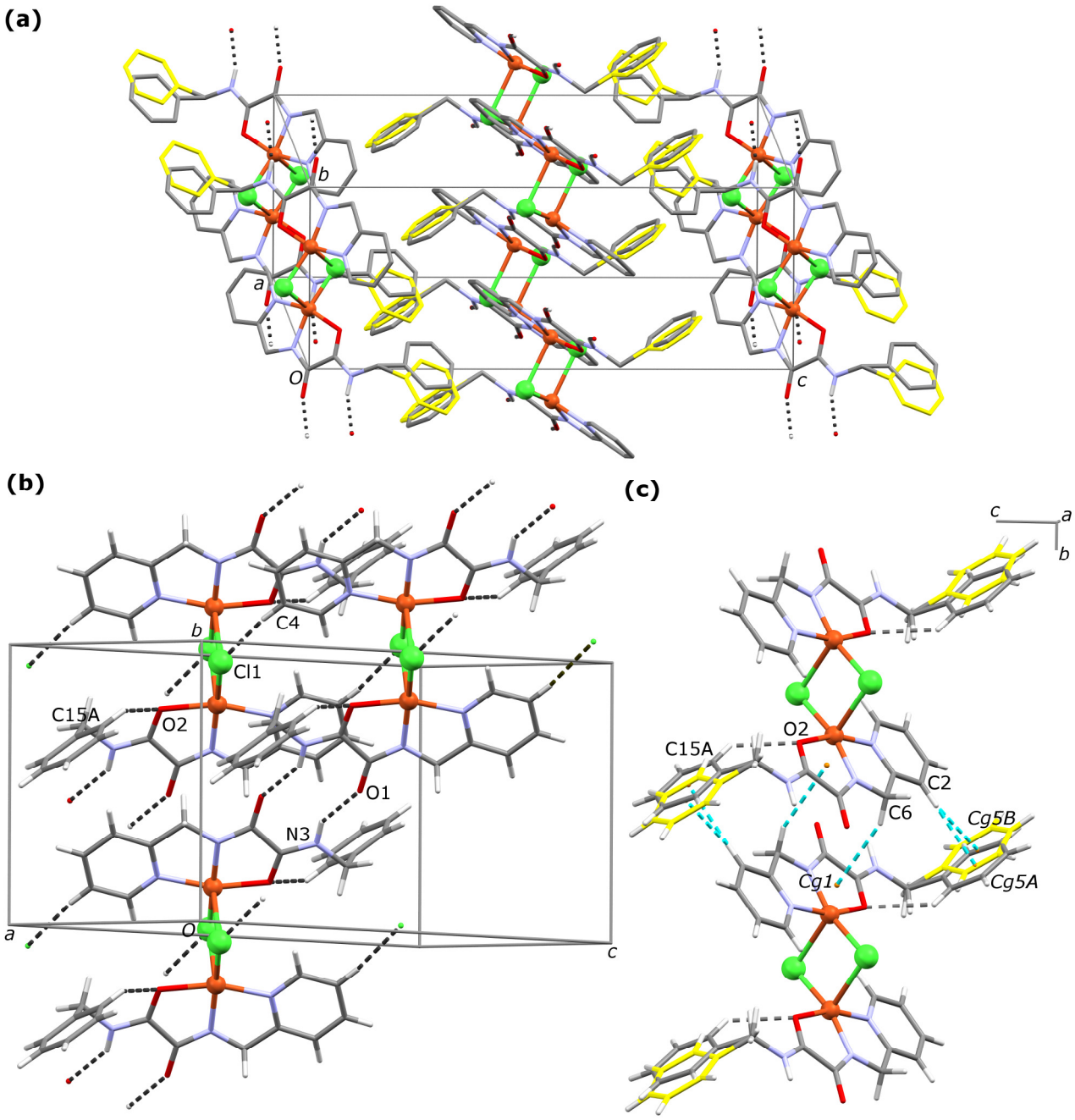

Fig. S9: Molecular packing in the crystal structure of **L^2–Cl**. (a) Supramolecular architecture allows the discrete disorder of *N*-benzyl groups. (b) In addition to the N–H···O hydrogen bonds, the C–H···O and C–H···Cl interactions are also present. (c) C–H···π interactions play a role in the molecular association. Minor conformation of the disordered *N*-benzyl group is depicted in yellow, except in (b) where it is omitted for clarity. *Cgn* denotes a centroid of the ring *n* as defined in Table 7. Interactions are represented as dashed lines in different colours: *cyan* for C–H···π interactions and *black* for other types of hydrogen bonding. H atoms bound to C atoms are omitted for clarity in (a). Cu and Cl atoms are shown as large spheres.

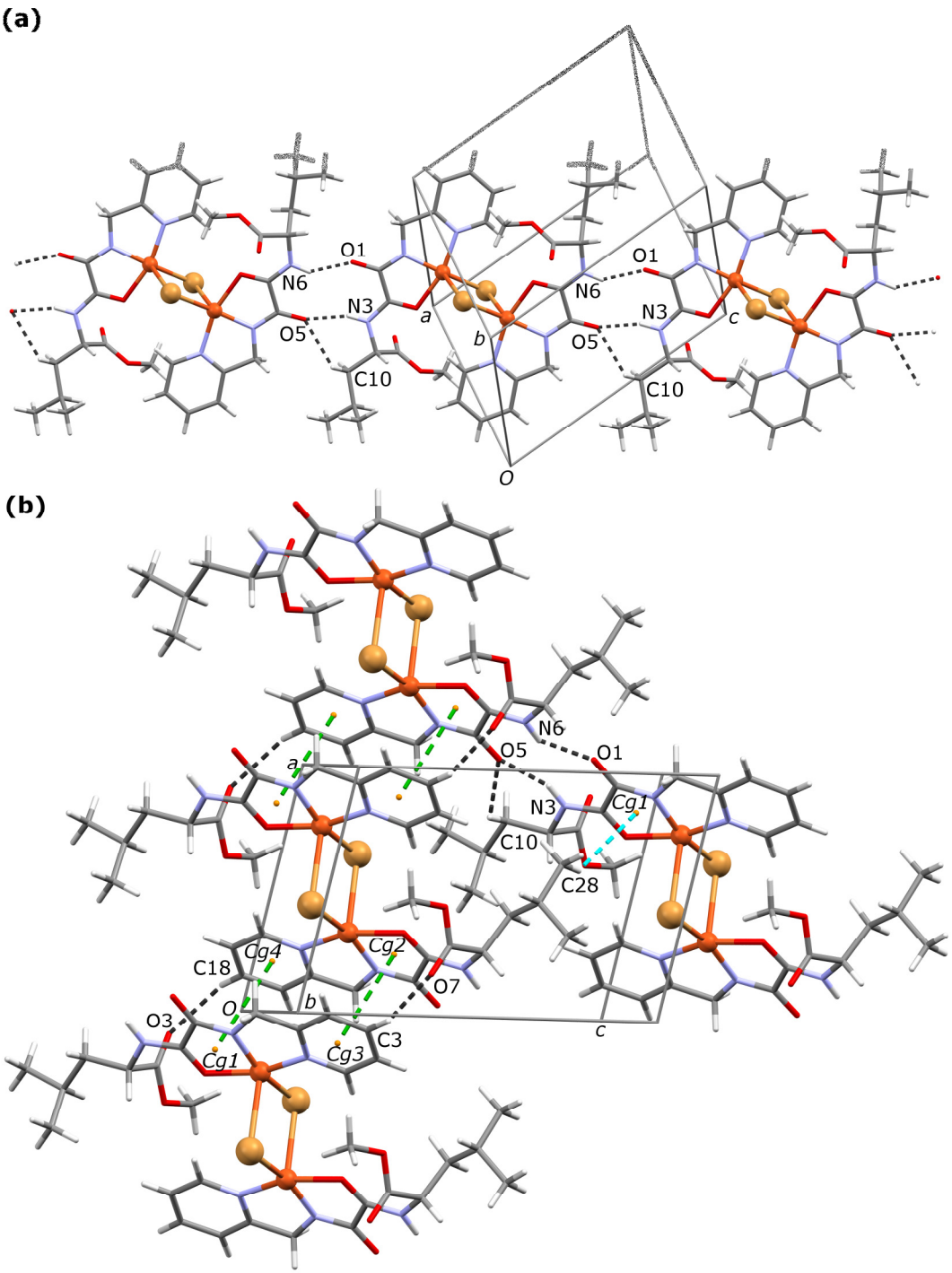

Fig. S10: Molecular packing in the crystal structure of **L^1–Br**. (a) An infinite chain of N–H····O hydrogen-bonded molecular dimers. (b) Stacking, C–H···π and C–H···O interactions. *Cgn* denotes a centroid of the ring *n* as defined in Table 6. Interactions are represented as dashed lines in different colours: *green* for the stacking interactions, *cyan* for a C–H···π interaction and *black* for other types of hydrogen bonding. Cu and Br atoms are shown as large spheres.

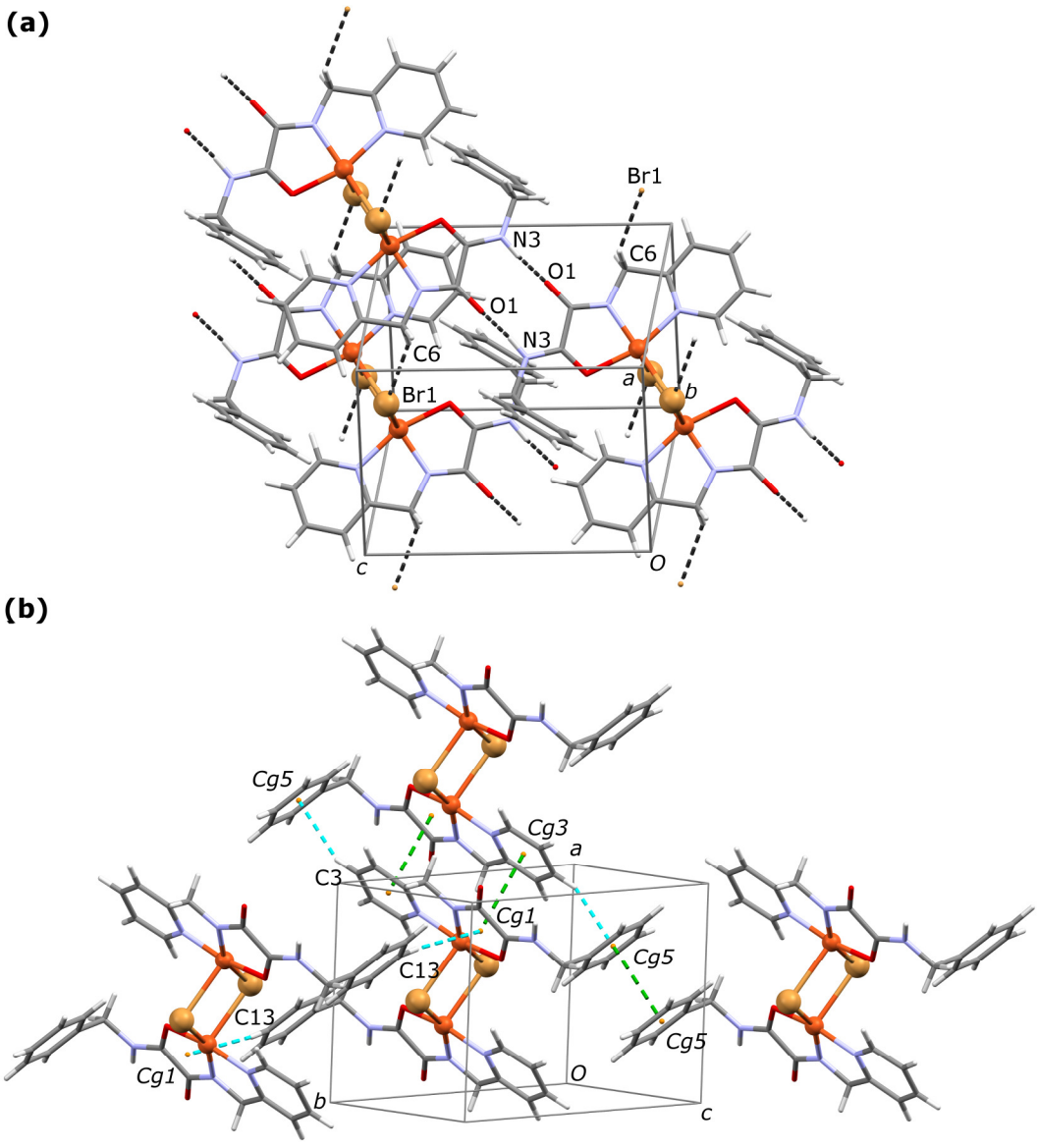

Fig. S11: Molecular packing in the crystal structure of $\mathbf{L^2}$**–Br**. (a) N–H···O and C–H···Br hydrogen bonds. (b) Stacking and C–H···π interactions. *Cgn* denotes a centroid of the ring *n* as defined in Table 6. Interactions are represented as dashed lines in different colours: *green* for the stacking interactions, *cyan* for C–H···π interactions and *black* for other types of hydrogen bonding. Cu and Br atoms are shown as large spheres.

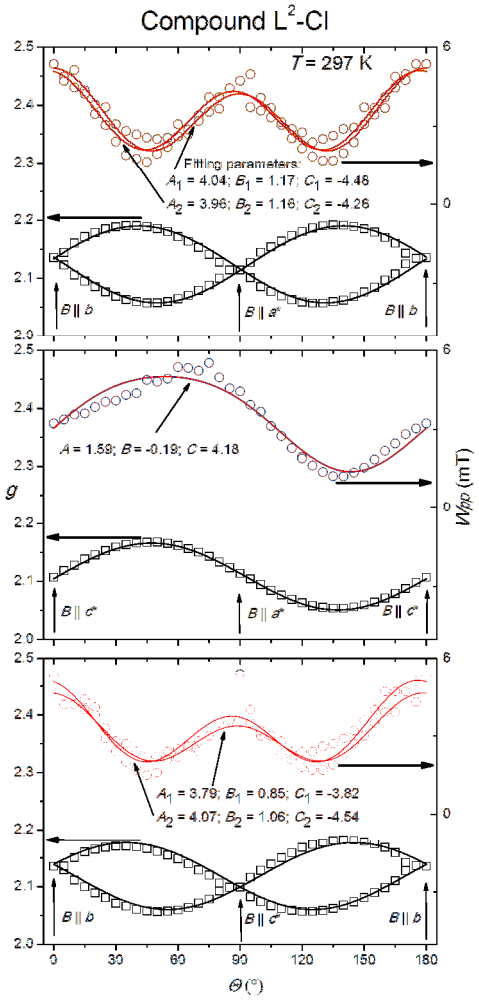

Fig. S12: Angular variation of the *g*-values (black squares) and the *Wpp* linewidths (red circles) of EPR lines for the single crystal of compound **L^2–Cl**, at room temperature, in three mutually perpendicular planes. Solid lines represent the fitted *g*-values with parameters given in Table 2 and *Wpp* linewidths with parameters given in the figure, according to eq. 1 and eq. 2, respectively.

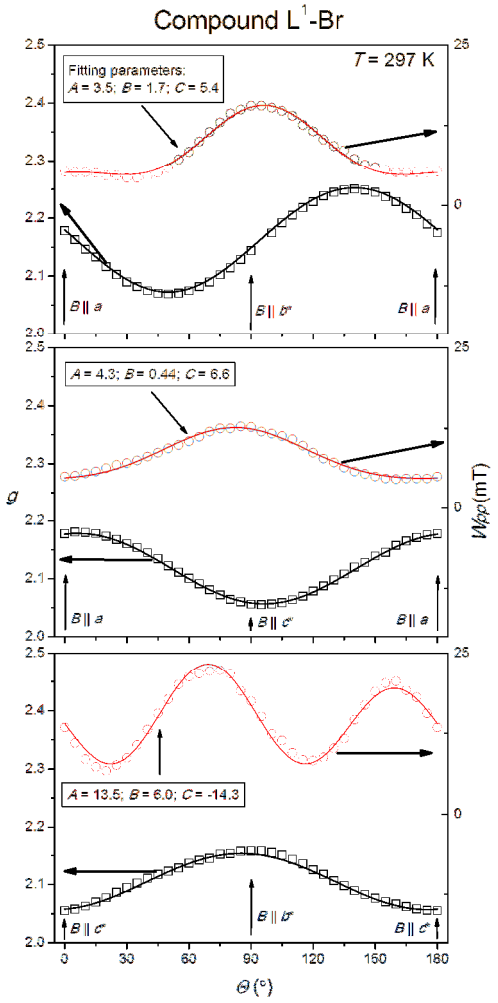

Fig. S13: Angular variation of the *g*-values (black squares) and the *Wpp* linewidths (red circles) of EPR lines for the single crystal of compound **L^1–Br**, at room temperature, in three mutually perpendicular planes. Solid lines represent the fitted *g*-values with parameters given in Table 2 and *Wpp* linewidths with parameters given in the figure, according to eq. 1 and eq. 2, respectively.

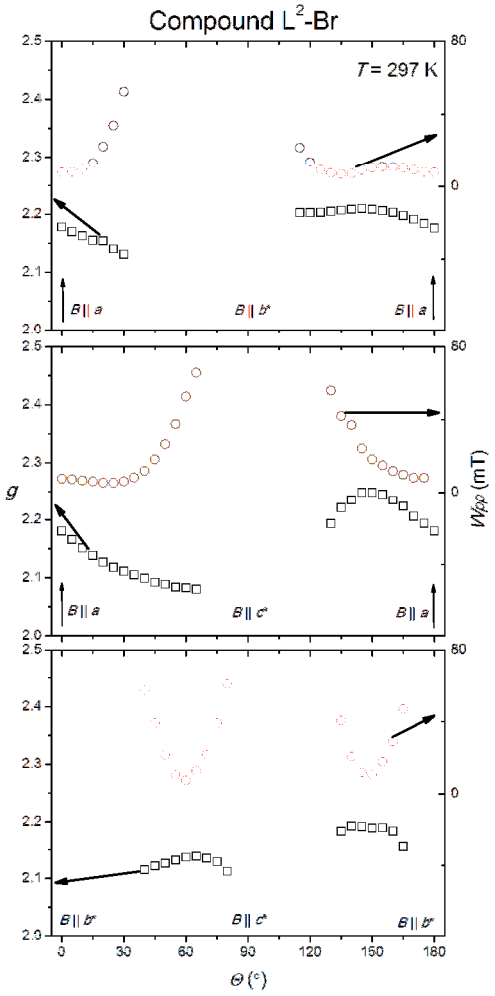

Fig. S14: Angular variation of the *g*-values (black squares) and the *Wpp* linewidths (red circles) of EPR lines for the single crystal of compound **L^2–Br**, at room temperature, in three mutually perpendicular planes. Some EPR lines were too weak and/or too broad to be detected.

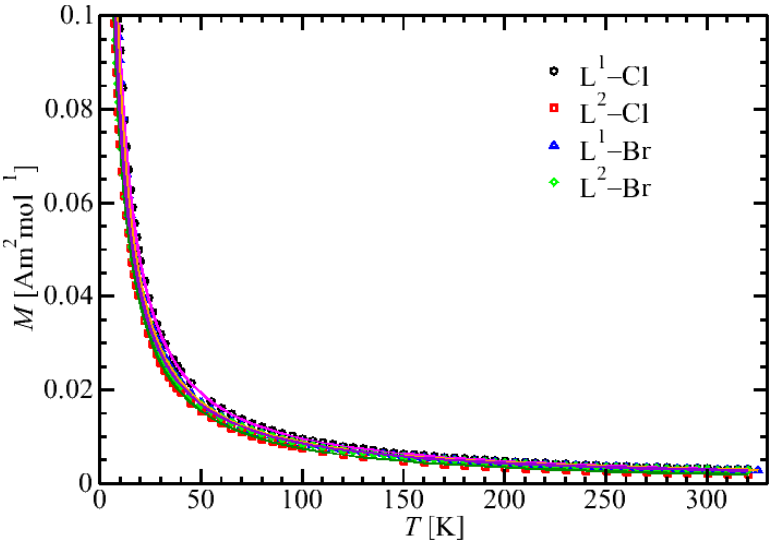

Fig. S15: Temperature dependence of magnetization, measured in field of 0.1 T. Lines are fitting curves using the Curie-Weiss model. We have obtained the following Curie constants (in emuK/molOe): 0.982(5), 0.829(3), 0.854(7) and 0.859(5), for complexes **L^1–Cl**, **L^2–Cl**, **L^1–Br** and **L^2–Br**, respectively. The resultant *g*-factors are 2.29(1), 2.10(1), 2.14(1) and 2.14(1) and Weiss parameters are –0.6(3)K, –1.3(7)K, –0.1(2)K, and –1.0(4)K, for **L^1–Cl**, **L^2–Cl**, **L^1–Br** and **L^2–Br**, respectively.

Table 8 Structural and magnetic properties for the selected dibromo-bridged copper(II) dimers

Compound[a]	Geometry	τ	$2J$ (cm^{-1})	Ref.
$[Cu(\alpha\text{-pic})_2Br_2]_2$	SP	0	-5	55
$[Cu(dmen)Br_2]_2$	SP	0.11	-2.4	30
$[Cu(dmgH)Br_2]_2$	SP	0.025	-3.02	56
$[Cu(4\text{-metz})_2Br_2]_2$	SP	0.045	-2.4	50
$[Cu(dien)Br_2]_2(ClO_4)_2$	SP	0.3	2.8	12
$[Cu(4\text{-meox})_2Br_2]_2$	SP	0.26	-15.2	57
$[Cu(terpy)Br]_2(PF_6)_2$	SP	0.24	-7.4	49
$[Cu(L^a)Br_2]_2$	SP	0.02;0.1	-11.76	10
$[Cu(L^b)Br]_2$	SP	0.03	-3.14	58
$[Cu(tmen)Br_2]_2$	SP	0.25	-4	54, 59
L^1–Br	SP	0.04;0.00	-0.14	this work
L^2–Br	SP	0.10	-2.36	this work
$[Cu(MAEP)Br_2]_2$	TBP	0.52	-4.3	60
$(3ap)_2[Cu_2Br_6]_2\cdot 2H_2O$	TBP	0.6	-53.8	61
$[Cu(dmtp)_2Br_2]_2\cdot 2H_2O$	TBP	0.62	-21.1	54

[a] Abbreviations: α-pic = α-picoline (2-methylpyridine); MAEP = 2-(2-(methylamino)ethyl)pyridine; dmen = *N*,*N*-dimethylethylenediamine; dmgH = dimethylglyoxime; 4-metz = 4-methylthiazole; dien = diethylenetriamine; 4-meox = 4-methyloxazole; terpy = 2,2':6',2"-terpyridine; L^a = 1,4-diazacycloheptane; HL^b = *N*-(1H-pyrrol-2-ylmethylene)-2-pyridineethanamine; tmen = *N*,*N*,*N'*,*N'*-tetramethylethylenediamine; 3ap = 3-aminopyridinium cation; dmtp = 5,7 dimethyl-1,2,4-triazolo[1,5-α]pyrimidine; SP = square pyramid and TBP = trigonal bipyramid.